Archives of Biochemistry and Biophysics
Vol. 364, No. 2, April 15, pp. 161–166, 1999
Article ID abbi.1999.1137, available online at http://www.idealibrary.com on IDEAL®

Interaction of Nickel(II) with Histones: *In Vitro* Binding of Nickel(II) to the Core Histone Tetramer

Wojciech Bal,*,† Vassiliki Karantza,‡ Evangelos N. Moudrianakis,‡ and Kazimierz S. Kasprzak*,[1]
*Laboratory of Comparative Carcinogenesis, National Cancer Institute, FCRDC, Frederick, Maryland 21702;
‡Department of Biology, Johns Hopkins University, Baltimore, Maryland 21218; and
†Faculty of Chemistry, University of Wroclaw, Wroclaw, Poland

Received September 8, 1998, and in revised form January 25, 1999

The absorption spectra of Ni(II) bound to the core histone tetramer, $(H3\text{-}H4)_2$, of chicken erythrocytes in 500 mM NaCl + 100 mM phosphate (pH 7.4) were recorded. A charge transfer band was seen at 317 nm, characteristic of a bond between Ni(II) and the sulfur atom of Cys-110 of histone H3. The conditional affinity constants for Ni(II) binding at pH 7.4 for low and high Ni(II) saturation (log K^c = 4.26 ± 0.02 and 5.26 ± 0.11 M^{-1}, respectively) were calculated from spectrophotometric titrations with the use of this band. The binding of Ni(II) to $(H3\text{-}H4)_2$ is proposed to involve the Cys-110 and His-113 of different H3 molecules within the tetramer. The competition between histones and low-molecular-weight chelators for Ni(II) in the cell nucleus, histidine and glutathione, is discussed on the basis of the above results, indicating that histone H3 is very likely to bind Ni(II) dissolved intracellularly from phagocytosed particulate nickel compounds. © 1999 Academic Press

Key Words: **nickel(II); nickel(II)–thiol coordination; histone H3; histone H4; core histone tetramer; association constant; UV–vis spectroscopy; charge transfer band.**

Nickel compounds are established human carcinogens (1). The molecular mechanisms underlying their activity, not fully understood, are believed to involve promutagenic DNA damage and epigenetic effects in chromatin resulting from Ni(II) binding to the cell nucleus (2–8). DNA polymer binds Ni(II) only weakly (2), leaving the proteins of the cell nucleus as likely Ni(II) targets. Histones are by far the most abundant among them. Therefore, if even moderate affinity Ni(II)-binding sites could be found in them, they might be able to compete for Ni(II) with even higher affinity sites in other, less abundant nuclear proteins or with smaller ligands, like histidine or glutathione. Consequently, detection and structural and mechanistic description of specific Ni(II) sites in histones would provide a molecular basis for better understanding of the mechanisms underlying Ni(II)-induced genotoxicity and carcinogenesis. This simple notion encouraged us to review the amino acid sequences of the histones (9, 10) in order to identify putative Ni(II) binding motifs and, subsequently, investigate the formation and physicochemical properties of Ni(II) complexes with those motifs.

Available information on the binding modes of Ni(II) to proteins (11) and data for nickel–peptide complexes (12, 13) indicate that His imidazoles and Cys thiols should be preferred by Ni(II) among donor groups provided by the amino acid residues of proteins. Carboxyl groups of Asp and Glu can play only secondary roles in the binding. As we found, the linker histone H1 does not contain any His or Cys residues. Furthermore, the crystal structure of the core histone octamer (14–18) indicates that the His residues, present in all core histones, and the Cys-96 residue of one of the variants of histone H3, remain isolated from each other in the three-dimensional structure. The two remaining possibilities for a specific binding site in the octamer are therefore the -ESHH- (residues 121–124 of H2A) and -CAIH-[2] (residues 110–113 of H3) motifs. The former is located in the C-terminal part of histone H2A. This

[1] To whom correspondence should be addressed at NCI-FCRDC, Building 538, Room 205, Frederick, MD 21702-1201. Fax: 301-846-5946.

[2] Abbreviations used: $(H3\text{-}H4)_2$, T, core histone tetramer; DTNB, 5,5′-dithiobis(2-nitrobenzoic acid); Hepes, *N*-(2-hydroxyethyl)piperazine-*N*′-2-ethanesulfonic acid; CT, charge transfer; CAIH, CH_3CO-Cys-Ala-Ile-His-NH_2; -CAIH-, the -Cys-Ala-Ile-His- sequence within the protein chain; K^c, conditional affinity constant; β, stability constant; GSH, reduced glutathione.

0003-9861/99 $30.00

part of the amino acid chain was not ordered enough to be seen in the crystal structures (14, 18). However, the positioning of the preceding residues of H2A indicates that it extends beyond the octamer core, forming a whisker that may interact with octamer-bound DNA (18). The -CAIH- moiety of histone H3, on the other hand, is located very close to the twofold symmetry axis of the octamer, and the distance between sulfur atoms from two H3 molecules is so short that they can easily form a disulfide bridge (17–19). This situation presents a possibility of formation of a binding site consisting of two -CAIH- units. Despite being located inside the molecule, the -CAIH- motif is accessible, as evidenced by a range of covalent modifications applied to Cys-110 in isolated octamers (20). Moreover, Cys-110 was a binding site for Hg(II) in octamer crystals used for crystallography (17, 18). All these facts point to the -CAIH- motif as a very likely Ni(II) binding site in the histone octamer. The hydrophobic environment in the protein interior is also expected to enhance Ni(II) binding (21–23).

Characterization of metal ion interactions with an object as complex as the core histone octamer is a difficult task. Therefore, we began our investigations with a "minimal" model, the N- and C-terminally blocked tetrapeptide, acetyl-Cys-Ala-Ile-His-amide (CAIH), aimed at reproducing local binding capabilities of the corresponding amino acid sequence of H3 (24) and evaluating the redox activity of the resulting complexes (25). This peptide was found to form distorted square-planar complexes, Ni(CAIH) and Ni(CAIH)$_2$, with Ni(II) ions bound through the Cys thiol and the His imidazole nitrogen (24). In the presence of phosphate ions, a strong ternary octahedral complex, Ni(H_2PO_4)(CAIH), was formed (25).

The next logical step of our studies was to find out whether the CAIH motif remained a Ni(II) binding site in the protein environment. In order to avoid possible competition from the -ESHH- site in histone H2A, instead of using the whole octamer, we chose to use first the core tetramer, (H3-H4)$_2$, of chicken erythrocytes. The present communication reports the results of this study. Characteristics of interactions of Ni(II) with the -ESHH- motif are presented separately (26).

MATERIALS AND METHODS

Materials. $NiCl_2$ (99.9999% purity) was purchased from Aldrich Chemical Co. (Milwaukee, WI). Chelex-100 chelating resin was purchased from Bio-Rad Laboratories (Richmond, CA); monosodium and disodium phosphates were obtained from Fisher Scientific (Fair Lawn, NJ); and NaCl, DTNB, Hepes, and urea were obtained from Sigma Chemical Co. (St. Louis, MO).

Sample preparation. Histone tetramers were isolated and purified as described previously (27, 28). Nickel binding experiments were performed in the following buffers: 500 mM NaCl + 100 mM phosphate, pH 7.4 (buffer A), and 10 mM Hepes, pH 7.4 (buffer B). Tetramer concentrations were determined spectrophotometrically, using A_{277} of 0.444 for a 1 mg/ml concentration (28, 29). The concentrations of SH groups were measured by reacting tetramers with DTNB in the presence of 4 M urea, as described previously (28). Between 95 and 98% of the tetramers was found to be in the reduced form. Three independent tetramer preparations were used for studies with each buffer.

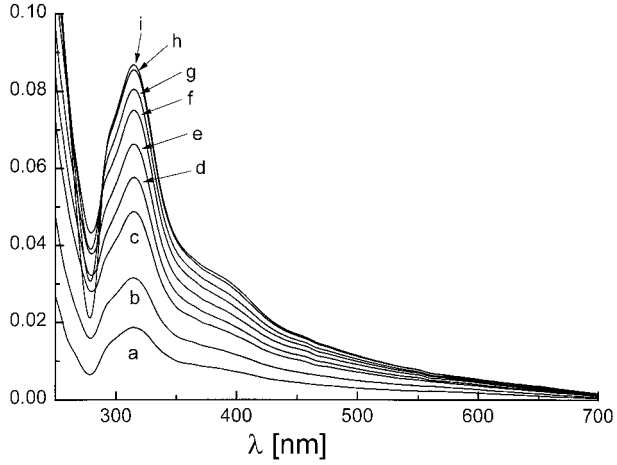

FIG. 1. Typical titration of (H3-H4)$_2$ with $NiCl_2$ in buffer A. Difference spectra, with the spectrum of nickel-free (H3-H4)$_2$ subtracted. For graphical clarity, not all spectra recorded (compare with Fig. 2) are shown. $NiCl_2$ equivalents: a, 2.7; b, 4.6; c, 6.4; d, 8.2; e, 9.9; f, 11.7; g, 16.1; h, 21.2; i, 31.3.

UV–vis spectra. The spectra were recorded at 25°C on a Beckman DU-640 spectrometer (Beckman Instruments, Palo Alto, CA), using reduced-volume 1-cm cells (Hellma Cells, Forest Hills, NY).

Affinity constant calculations. The conditional affinity constant K^c for Ni(II) binding to (H3-H4)$_2$ was calculated from relations between the A_{317} values and Ni(II) and protein thiol group concentrations. The saturation values of A_{317} were assumed to correspond to 100% binding in respect to protein. A 1:1 stoichiometry between Ni(II) and the tetramer was assumed, leading to the expression for the conditional affinity constant at pH 7.4: $K^c = [NiT]/[Ni^{2+}][T]$, where T stands for (H3-H4)$_2$. The values for [NiT]/[T] were obtained from titration curves. Formation of a $NiHPO_4$ complex is a process competitive to the (H3-H4)$_2$ Ni(II) binding, thus affecting the value of $[Ni^{2+}]$ in the expression for K^c. Appropriate corrections were calculated from phosphate protonation and stability constants presented in Ref. (25) (see Appendix for derivation).

RESULTS

The addition of 0.5 equivalents of nickel chloride to (H3-H4)$_2$ solutions in buffer A resulted in the appearance of a new absorption band with a maximum at 317 nm in UV–vis spectra. With further $NiCl_2$ additions, its intensity increased. At about 3 $NiCl_2$ equivalents, increased light scattering was evident, but the difference spectra indicated that the specific 317-nm band continued to intensify until saturation was observed at 25–30 nickel equivalents (Fig. 1). After each $NiCl_2$ addition, spectra were recorded repeatedly and difference spectra were checked for the increase of the 317-nm band. The state of equilibrium, with respect to this band, was seen within 15 min for the lower part of the titration

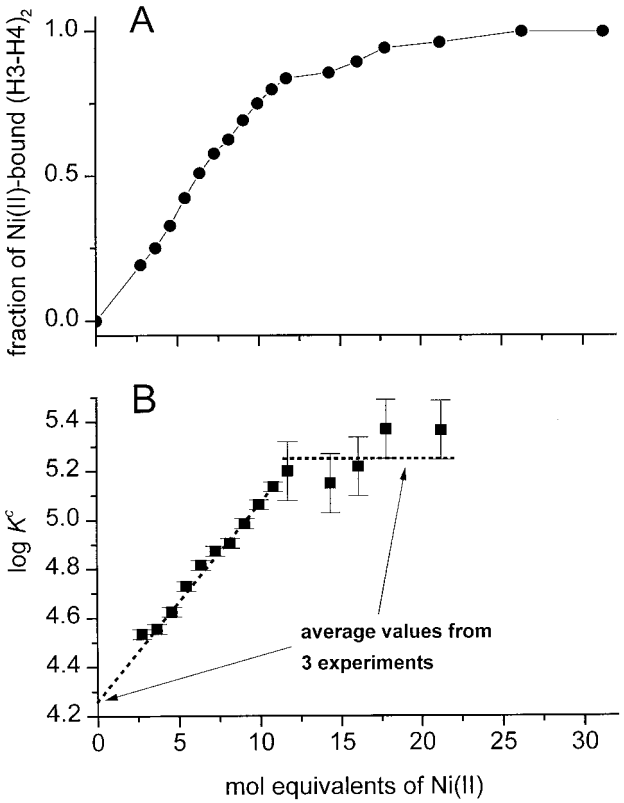

FIG. 2. (A) A_{317} values from a typical titration of $(H3\text{-}H4)_2$ with $NiCl_2$ in buffer A, normalized to the saturation value. (B) Values of log K^c corresponding to the titration presented in A.

curve and within 5 min for the upper part. The scatter correction was achieved with the use of reference curves, obtained for control samples of nickel-free tetramers which aggregate in solution upon standing (29). The loss of protein from solution during the titrations, resulting from aggregation, did not exceed 4% of the initial concentration. This loss did not have any considerable impact on the affinity constant calculations.

With buffer B, the addition of the first 1–1.5 equivalents of nickel yielded spectral changes similar to those seen with buffer A. However, further addition of $NiCl_2$ contributed only to the 390-nm band of Ni(II) phosphate complexes.

Figure 2A presents an example of a titration curve obtained from the light scatter-corrected spectra. Such curves were used to calculate the affinity constant for Ni(II) binding to $(H3\text{-}H4)_2$. A stoichiometry of one Ni(II) ion per $(H3\text{-}H4)_2$ was assumed (see below). As seen in Fig. 2B, the value of K^c initially increases linearly with the amount of Ni(II) added, reaching a plateau at and above 75% of saturation. Table I presents the values of the affinity constant obtained from three independent experiments for high saturation (using the upper segments of titration curves) as well as

TABLE I

Conditional Affinity Constant (K^c) for Ni(II) Binding to $(He\text{-}H4)_2$ at pH 7.4 in High-Ionic-Strength Solution (0.1 M Na Phosphate Buffer + 0.5 M NaCl)[a]

Experiment	Tetramer concentration (μM)	log K^c ± SD	
		High saturation	Low saturation
1	33.5	5.33 ± 0.12	4.27 ± 0.02
2	23.3	5.22 ± 0.10	4.26 ± 0.02
3	24.6	5.24 ± 0.10	4.26 ± 0.02
1 + 2 +3		5.26 ± 0.11	4.26 ± 0.02
CAIH[b]		2.79	

[a] $K^c = [NiT]/[Ni^{2+}][T]$, $T = (H3\text{-}H4)_2$; K^c unit is M^{-1}.
[b] Recalculated from the data in Refs. (24) and (25), using $\log K^c = \log \beta_{Ni(CAIH)} - \log(1 + [H^+]\beta_{HL} + [H^+]^2\beta_{H2L})$, equal to $\log \beta_{Ni(CAIH)} - 1.25$ at pH 7.4.

for low saturation (extrapolating the linear segments to zero concentration of Ni(II) ions).

Figure 3 presents the spectrum resulting from Ni(II) binding to the $(H3\text{-}H4)_2$ compared to the spectrum of the Ni(II) complex with CAIH (24, 25). The 317-nm band is a charge transfer (CT) between Ni(II) and thiol sulfur in a square-planar complex (24, 30), and therefore the unique Cys-110 is the binding site for Ni(II) in the tetramer. Extensive formation of this band was seen in buffer A, which stabilizes $(H3\text{-}H4)_2$ tetramers, as opposed to buffer B, in which the equilibrium is shifted toward H3-H4 heterodimers (29). Therefore, the conformational effect of the tetrameric assembly is required to form a specific, sterically accessible binding site at the -CAIH- motif.

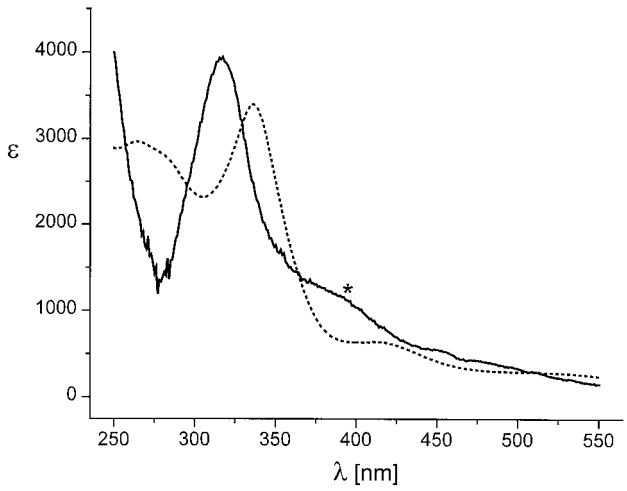

FIG. 3. The absorption spectrum of the Ni(II) complex of $(H3\text{-}H4)_2$ (solid line) compared to the spectrum of Ni(CAIH) (dashed line). The asterisk marks the band of the octahedral $NiHPO_4$ complex, which exists in equilibrium with the Ni(II)–$(H3\text{-}H4)_2$ complex.

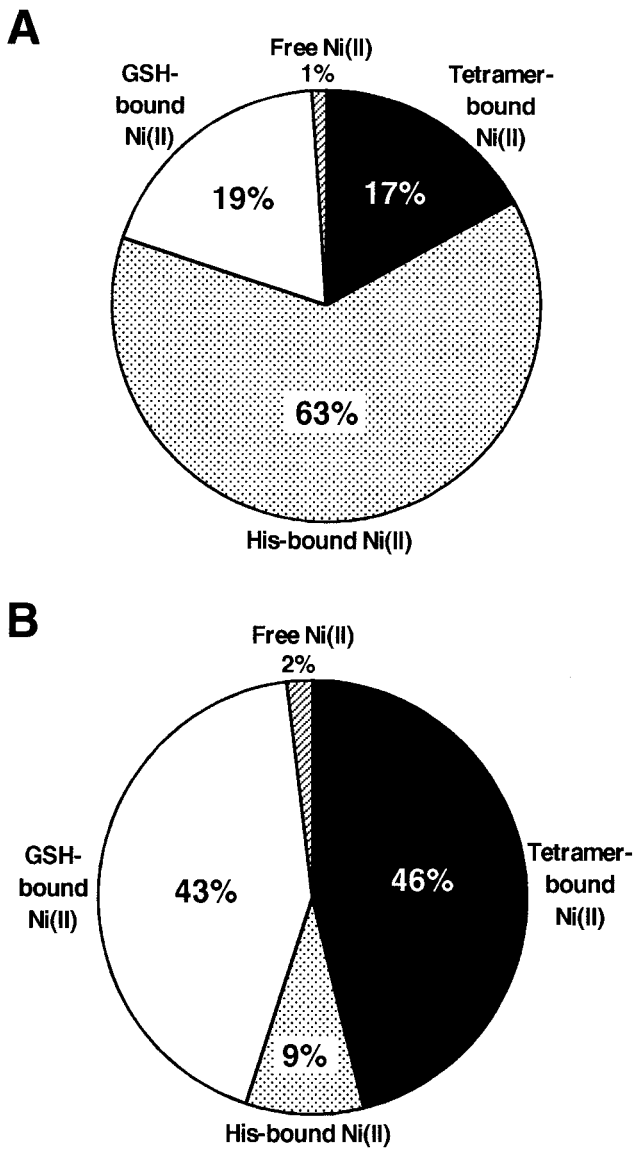

FIG. 4. Hypothetical speciation of Ni(II) (A, 0.1 mM; B, 1 mM) between 1.6 mM $(H3\text{-}H4)_2$, 1 mM GSH, and 0.1 mM His at pH 7.4. Calculations were made using an in-house written computer program based on algorithms from the SUPERQUAD package (36). The concentration of the tetramer in the nucleus, 1.6 mM, was determined based on the volume of the human hepatocyte nucleus of 300 μm^3, DNA length of 6×10^9 bp, and the presence of one histone octamer per 200 bp (37). Stability constants for GSH–Ni(II) complexes were taken from Ref. (32), and those for His–Ni(II) complexes were taken from Ref. (34).

The model Ni(CAIH) complex easily coordinated phosphate ions that resulted in the formation of an octahedral species (25). This does not happen in the tetramer. Also, the CT band in the $(H3\text{-}H4)_2$ complex is blueshifted by 15 nm compared to the peptide model. Another difference is in the rate of complexation: The peptide complex forms instantaneously (24, 25), whereas the binding to the tetramer takes several minutes. The addition of sub-millimolar concentrations of $NiCl_2$ resulted in increased aggregation of tetramers, as reflected by the increase of light scattering, which in turn enhanced Ni(II) binding. Previous studies (29) indicated that the aggregation of histone tetramers in chloride-containing solutions correlated with increased contents of the α-helix. This effect does not alter the complex structure, because its CT spectrum remains unchanged, but it increases its stability as titration progresses. The bottom line of Table I contains the value of log K^c of the Ni(CAIH) complex, calculated from the data presented in Ref. (25). Comparison of this value with those obtained for the tetramer indicates that at pH 7.4 Ni(II) binds to $(H3\text{-}H4)_2$ ca. 30 times more strongly than to the model CAIH tetrapeptide and that tetramer aggregation further increases the binding affinity by a factor of 10.

DISCUSSION

The above described features of Ni(II) binding to $(H3\text{-}H4)_2$ can be explained in the following way: Due to the constraints resulting from the secondary structure of the $(H3\text{-}H4)_2$ at the -CAIH- sequence (16–18), the simultaneous binding of His and Cys residues from the same H3 molecule is impossible; hence, there is little binding at low ionic strength (buffer B), i.e., under conditions favoring H3-H4 dimers. In the $(H3\text{-}H4)_2$ tetramer the binding of a Ni(II) ion to a Cys residue from one H3 and a His or Cys residue from another is possible but imposes strain on the protein fold. The 30-fold stability gain vs the model CAIH peptide complex is likely to result from the hydrophobic shielding in the protein interior (21–23). The association of histone tetramers into larger aggregates (29), facilitated by excess Ni^{2+} ions, changes the protein conformation slightly, reducing this strain and therefore increasing complex stability (elevation of log K^c from 4.26 to 5.26). Both a blueshift of the CT band and a slower binding, compared to the CAIH peptide model, may indicate a more regular square-planar structure of the complex. An alternative Ni(II) binding mode in the tetramer (especially in its aggregates), with Cys sulfurs of two H3 histones both coordinated in a *cis* arrangement, cannot be ruled out, either.

Reduced glutathione (GSH), present in the nuclei at millimolar concentrations, has been implied as a protective agent against nickel toxicity (31). It forms stable complexes with Ni(II) (32). Histidine, present in body fluids at 0.1 mM concentrations (33), forms very strong Ni(II) complexes *in vitro* (34) and therefore might also compete for Ni(II) binding *in vivo*, despite its lower concentration. In order to estimate the biological importance of Ni(II) binding to histones in the cell nucleus, we calculated the hypothetical speciation at pH 7.4 between $(H3\text{-}H4)_2$ and these two potential

Ni(II) ligands in the cell. The results of these calculations, presented in Fig. 4, suggest that histidine rather than glutathione might be a major intracellular Ni(II) chelator at low levels of exposure. However, higher intracellular Ni(II) concentrations are likely to occur intracellularly due to phagocytosis and dissolution of particulate nickel compounds which are main human carcinogens (35). Under such conditions, the -CAIH- binding site in histone H3 emerges as a likely target for nickel in the cell nucleus. This binding must therefore be taken into account in consideration of molecular mechanisms of nickel genotoxicity and carcinogenesis. In fact, our results set the lower limit for Ni(II) affinity to core histones, because they do not include the Ni(II) binding to histone H2A, the presumed caging effects of octamer formation, and the electrostatic stabilization by DNA of the Ni(II) binding to the -CAIH- site in nucleosome. The nucleosomal destabilization through an alteration of the H3 surface in the vicinity of the dyad (38, 39) is a potential deleterious effect of Ni(II) binding. The study of this effect is a goal of our further studies.

APPENDIX

Calculation of Affinity Constant, K^c

C_T, total concentration of $(H3\text{-}H4)_2$.
C_{Ni}, total concentration of Ni(II).
X, fraction of $(H3\text{-}H4)_2$ forming Ni(II) complex.
phos, total concentration of phosphate.
β_p, stability constant for $NiHPO_4$.
β_i, respective protonation constants for phosphate ions, $i = 1, 2, 3$.

$$K^c = [NiT]/[T][Ni^{2+}] = X/(1 - X) \times 1/[Ni^{2+}];$$
$$[Ni^{2+}] = C_{Ni} - [NiT] - [NiHPO_4]$$
$$[NiHPO_4] = \beta_p[Ni^{2+}][H^+][PO_4^{3-}]$$
$$[Ni^{2+}] = C_{Ni} - XC_T - \beta_p[Ni^{2+}][H^+][PO_4^{3-}];$$
$$[Ni^{2+}] = (C_{Ni} - XC_T)/(1 + \beta_p[H^+][PO_4^{3-}])$$
$$\text{phos} = [PO_4^{3-}] + [HPO_4^{2-}] + [H_2PO_4^-] + [H_3PO_4] + [NiHPO_4] = [PO_4^{3-}](1 + \beta_1[H^+] + \beta_2[H^+]^2 + \beta_3[H^+]^3 + \beta_p[H^+][Ni^{2+}])$$

At $C_{Ni} \ll$ phos, the $[NiHPO_4]$ contribution to total phosphate concentration becomes negligible, yielding: $[Ni^{2+}] = (C_{Ni} - XC_T)(1 + \beta_1[H^+] + \beta_2[H^+]^2 + \beta_3[H^+]^3)/(\beta_p [H^+]$ phos), and $K^c = \{X/(1 - X)\} \times (\beta_p[H^+]\text{phos})/(C_{Ni} - X C_T)(1 + \beta_1[H^+] + \beta_2[H^+]^2 + \beta_3[H^+]^3)$.

At pH 7.4 and phos = 0.1 M, $K^c = 8.179 \times \{X/(1 - X)(C_{Ni} - XC_T)\}$.

REFERENCES

1. IARC (1990) IARC Monographs on the Evaluation of Carcinogenic Risk to Humans, Vol. 49, Chromium, Nickel and Welding, IARC, Lyon.
2. Lee, J. E., Ciccarelli, R. B., and Wetterhahn Jennette, K. (1982) *Biochemistry* **21,** 771– 778.
3. Kasprzak, K. S., Waalkes, M. P., and Poirier, L. A. (1986) *Toxicol. Appl. Pharmacol.* **82,** 336–343.
4. Kasprzak, K. S. (1995) *Cancer Invest.* **13,** 411–430.
5. Costa, M. (1991) *Annu. Rev. Pharmacol. Toxicol.* **31,** 321–337.
6. Salnikow, K., Cosentino, S., Klein, C., and Costa, M. (1994) *Mol. Cell. Biol.* **14,** 851–858.
7. Lee, Y.-W., Klein, C. B., Kargacin, B., Salnikow, K., Kitahara, J., Dowjat, K., Zhitkovich, A., and Costa, M. (1995) *Mol. Cell. Biol.* **15,** 2547–2557.
8. Hartwig, A. (1995) *BioMetals* **8,** 3–11.
9. GenPept (GenBank Gene Products) Database distributed by National Cancer Institute, Frederick Biomedical Supercomputing Center. For GenBank, cf. Burks, C., Cassidy, M., Cinkosky, M. J., Cumella, K. E., Gilna, P., Hayden, J. E-D., Kelley, T. A., Kelly, M., Kristofferson, D., and Ryals, J. (1991) *Nucleic Acids Res.* **19**(Suppl.), 2221–2225.
10. von Holt, C., Brandt, W. F., Greyling, H. J., Lindsey, G. G., Retief, J. D., Rodrigues, J. A., Schwager, S., and Sewell, B. T. (1989) *in* Methods in Enzymology, Vol. 170, Nucleosomes (Wassarman, P. M., and Kornberg, R. D., Eds.), pp. 503–523, Academic Press, San Diego.
11. Halcrow, M. A., and Christou, G. (1994) *Chem. Rev.* **94,** 2421–2481.
12. Pettit, L. D., Gregor, J. E., and Kozlowski, H., (1991) *in* Perspectives on Bioinorganic Chemistry (Hay, R. W., Dillworth, J. R., and Nolan, K. B., Eds.), Vol. 1, pp. 1–41, JAI Press, Greenwich, CT.
13. IUPAC Stability Constants Database, Release 2 (1995) IUPAC and Academic Software.
14. Arents, G., Burlingame, R. W., Wang, B.-C., Love, W. E., and Moudrianakis, E. N. (1991) *Proc. Natl. Acad. Sci. USA* **88,** 10148–10152.
15. Arents, G., and Moudrianakis, E. N. (1994) *in* Structural Biology: The State of the Art, Proceedings of the Eighth Conversation, State University of New York, Albany, NY, 1993 (Sarma, R. H., and Sarma, M. H., Eds.), pp. 93–108, Adenine Press, New York.
16. Arents, G., and Moudrianakis, E. N. (1995) *Proc. Natl. Acad. Sci. USA* **92,** 11170–11174.
17. Wang, B.-C., Rose, J., Arents, G., and Moudrianakis, E. N. (1994) *J. Mol. Biol.* **236,** 179–188.
18. Luger, K., Mader, A. W., Richmond, R. K., Sargent, D. F., and Richmond, T. J. (1997) *Nature* **389,** 251–260.
19. Camerini-Otero, R. D., and Felsenfeld, G. (1977) *Proc. Natl. Acad. Sci. USA* **74,** 5519–5523.
20. Daban, J.-R., and Cantor, C. R. (1989) *in* Methods in Enzymology, Vol. 170, Nucleosomes (Wassarman, P. M., and Kornberg, R. D., Eds.), pp. 192–214, Academic Press, San Diego.
21. Bal, W., Chmurny, G. N., Hilton, B. D., Sadler, P. J., and Tucker, A. (1996) *J. Am. Chem. Soc.* **118,** 4727–4728.
22. Yamashita, M. M., Wesson, L., Eisenman, G., and Eisenberg, D. (1990) *Proc. Natl. Acad. Sci. USA* **87,** 5648–5652.
23. Regan, L. (1993) *Annu. Rev. Biophys. Biomol. Struct.* **22,** 257–281.
24. Bal, W., Lukszo, J., Jezowska-Bojczuk, M., and Kasprzak, K. S. (1995) *Chem. Res. Toxicol.* **8,** 683–692.
25. Bal, W., Lukszo, J., and Kasprzak, K. S. (1996) *Chem. Res. Toxicol.* **9,** 535–540.
26. Bal, W., Lukszo, J., Bialkowski, K., and Kasprzak, K. S. (1998) *Chem. Res. Toxicol.* **11,** 1014–1023.
27. Eickbush, T. H., and Moudrianakis, E. N. (1978) *Biochemistry* **17,** 4955–4964.

28. Feinstein, D. L., and Moudrianakis, E. N. (1986) *Biochemistry* **25,** 8409–8418.
29. Baxevanis, A. D., Godfrey, J. E., and Moudrianakis, E. N. (1991) *Biochemistry* **17,** 8817–8823.
30. Kozlowski, H., Decock-Le Reverend, B., Ficheux, D., Loucheux, C., and Sovago, I. (1987) *J. Inorg. Biochem.* **29,** 187–197.
31. Lynn, S., Yew, F. H., Hwang, J.-W., Tseng, M.-J., and Jan, K. Y. (1994) *Carcinogenesis* **15,** 2811–2816.
32. Formicka-Kozlowska, G., May, P. M., and Williams, D. R. (1980) *Inorg. Chim. Acta* **46,** L51–L53.
33. Altman, P. A., and Dittmer, D. S. (Eds.) (1961) Biology Data Book, Vol. 3, pp. 1805–1814, FASEB, Washington, DC.
34. Pettit, L. D. (1984) *Pure Appl. Chem.* **56,** 247–292.
35. Evans, R. M., Davies, P. J. A., and Costa, M. (1982) *Cancer Res.* **42,** 2729–2735.
36. Gans, E., Sabatini, A., and Vacca, A. (1985) *J. Chem. Soc. Dalton Trans.* 1195–1199.
37. Alberts, D., Bray, D., Lewis, J., Raff, M., Roberts, K., and Watson, J. D. (1994) Molecular Biology of the Cell, 3rd ed., pp. 335–399, Garland, New York.
38. Kurumizaka, H., and Wolffe, A. P. (1997) *Mol. Cell. Biol.* **17,** 6953–6969.
39. Hamiche, A., and Richard-Foy, H. (1998) *J. Biol. Chem.* **273,** 9261–9269.